Talanta 130 (2014) 307–314

Contents lists available at ScienceDirect

Talanta

journal homepage: www.elsevier.com/locate/talanta

Short communication

A uniform nonlinearity criterion for rational functions applied to calibration curve and standard addition methods

Anna Maria Michałowska-Kaczmarczyk [a], Agustin G. Asuero [b], Julia Martin [b], Esteban Alonso [b], Jose Marcos Jurado [b], Tadeusz Michałowski [c,*]

[a] Department of Oncology, The University Hospital in Cracow, 31-501 Cracow, Poland
[b] Department of Analytical Chemistry, The University of Seville, 41012 Seville, Spain
[c] Faculty of Engineering and Chemical Technology, Technical University of Cracow, Warszawska 24, 31-155 Cracow, Poland

ARTICLE INFO

Article history:
Received 2 February 2014
Accepted 22 April 2014
Available online 10 May 2014

Keywords:
Chemical analysis
Calibration
Standard addition
Curve fitting
Rational functions

ABSTRACT

Rational functions of the Padé type are used for the calibration curve (CCM), and standard addition (SAM) methods purposes. In this paper, the related functions were applied to results obtained from the analyses of (a) nickel with use of FAAS method, (b) potassium according to FAES method, and (c) salicylic acid according to HPLC-MS/MS method. A uniform, integral criterion of nonlinearity of the curves, obtained according to CCM and SAM, is suggested. This uniformity is based on normalization of the approximating functions within the frames of a unit area.

1. Introduction

The nonlinear functions of variable x, applied for modeling made in many branches of applied sciences, are usually approximated over a limited part of its domain. Among various approximation methods, two are of particular interest: (1) the polynomial models based on Maclaurin's series expansion and (2) the model based on the rational functions called as Padé approximants [1–3], expressed by a quotient $P_n(x)/Q_m(x)$ of two polynomials $P_n(x)$ and $Q_m(x)$, with degrees m and n. The Padé function [4–6].

$$y = y_0(x; n, m) = \frac{\sum_{k=0}^{n} a_k x^k}{1 + \sum_{l=1}^{m} a_{n+l} x^l} = \frac{a_0 + \sum_{k=1}^{n} a_k x^k}{1 + \sum_{l=1}^{m} a_{n+l} x^l} \quad (1)$$

is applied for the calibration curve method (CCM). At $a_0=0$, from Eq. (1) we obtain the function

$$y = y_1(x; n, m) = \frac{\sum_{k=1}^{n} a_k x^k}{1 + \sum_{l=1}^{m} a_{n+l} x^l} \quad (2)$$

applicable for a standard addition method (SAM). As a rule, the functions (1) and (2) express the relationships between analytical signals (y) and concentrations (x) of an analyte. However, when referred to titrimetric methods of analysis, the roles of x and y are usually interchanged.

The fit of approximating functions: (1) and (2) to experimental points $\{(x_j, y_j)|j=1,\ldots,N\}$ is of primary importance in SAM and CCM. Rational function provides better approximation to experimental points $\{(x_j, y_j)|j=1,\ldots, N\}$ than polynomial functions. An illustration/proof of this property is the fit of polynomial and rational functions to the function $y = \ln(1+x) = \sum_{k=0}^{\infty}(-1)^{k+1}x^{k+1}/(k+1)$, shown in Fig. 1. Among others, the function [7]

$$y = \frac{2x}{2+x} \quad (3)$$

as a particular case of one-parametric relationship $y=y_1(x; 1,1)=ax/(1+ax)$ $(=x/(b+x), b=1/a)$, appears to be better than extension of $\ln(1+x)$ into Maclaurin's series up to 15th component [8], at $x=1$. The function (3) has been widely applied in modifications of the Gran I method [7–11]. Approximation $e^x=(2+x)/(2-x)$ was applied in [12]. More extended functions of the Padé type (Eq. (2)) were applied for modeling pH titration curves in the systems of concentrated electrolytes [13–19], where: $x=h$ – activity of H^+ ions, $pH=-\log h$, $y=W=V_0+V$; V_0 – volume of titrand (D), V – volume of titrant (T) added into D at a particular point of titration. In context with Eq. (2), it should be noted that the common titration is a kind of SAM, although T in [13–17] contained a standardized solution, together with a sample tested and a basal electrolyte. In [17–19], a function of the Padé type was presented as a sum of simple rational functions, of $a_i/(x+b_i)$ type; similar transformation (with Simms' constants involved) was used later in [20,21] for calculation of total alkalinity. Using rational functions requires nonlinear regression [4] and then analytical and physicochemical problems involved with Padé approximants were resolved there according to iterative procedures [22,23].

* Corresponding author. Tel.: +48 12 628 21 77.
E-mail address: michalot@o2.pl (T. Michałowski).

http://dx.doi.org/10.1016/j.talanta.2014.04.067
0039-9140/

Notations

CCM calibration curve method
LSM least squares method
SA salicylic acid
SAM standard addition method

As stated above, the rational functions with fewer number of coefficients give better approximation than the corresponding polynomial functions [4,24]. Rational functions are particularly applicable when strongly unsymmetrical dependences occur [25,26]. The Padé approximants are perceived as an accurate tool in some extrapolation procedures [27]; this property is particularly valuable in the context with SAM.

Rational functions were used for modeling enzyme-catalyzed reactions [28], and for ridge regression [29], where linear terms were introduced in numerator and denominator of the rational function in a kinetic model applied for esterification of ethanol with acetic acid. Another kind of rational function was applied [30] for flame atomic absorption spectrometry (FAAS) purposes. The Padé approximants were also considered as a flexible tool used for modeling adsorption data [31,32], for optimizing sugar production [26], scanning electrochemical microscopy [33], and handling the data related to mass transfer at microelectrodes [34,35].

A new formulation involved with rational functions and applied to SAM and CCM, has been presented recently [36,37]; it was proved that the functions $y=y_1(x; 2,1)$ and $y=y_1(x; 2,2)$ (see Eq. (2)) provide the results of FAAS analysis much more accurate than ones obtained with use of parabolic function [38], $y=y_1(x; 2,0)$. What is more, the functions $y=y_1(x; 2,1)$ and $y=y_1(x; 2,2)$ appeared to be robust against an effect of the matrix change, resulting from the addition of the standard solutions that changed a volume of the solution up to ca. 30% (the dilution effect was included in the model applied in [36]). This way, omission of one of the basic assumptions applied in SAM did not cause a deterioration of the accuracy of determinations, although SAM is commonly considered as a last resort rather than the method of choice [39].

In this paper, an effect of m in $y=y_0(x; 2,m)$ (see Eq. (2), $n=2$) on the fit of the related approximating functions to experimental points $(x_j, y_j)\ |j=1,\ldots,N\}$, expressed by the differences $\delta_j=y_j-y_0(x_j; 2,m)$, is indicated on an example of CCM applied for nickel determination according to FAAS method. Then nonlinear models derived for SAM were applied for results of analyses of potassium in a wine, and performed according to flame atomic emission spectrometry (FAES), widely used for determination of sodium and potassium in biological fluids [40–42]. The nonlinear model applied in SAM is referred here to the manner of preparation of analyzed samples (working solutions), different from the one applied in [36].

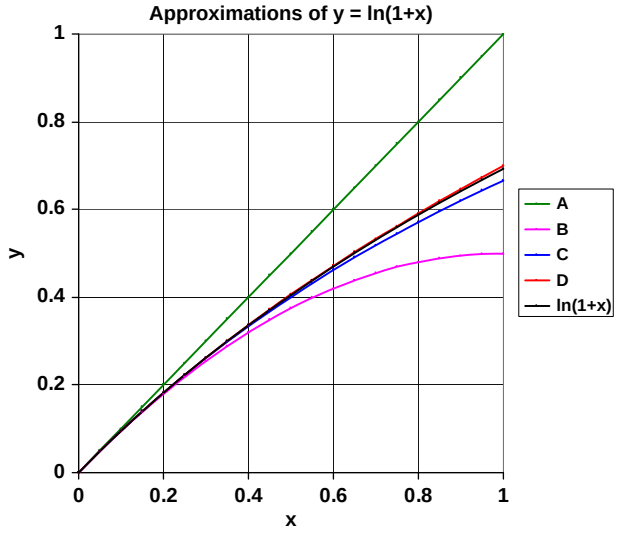

Fig. 1. Comparative plots of functions: (A) $y=x$, (B) $y=x-x^2/2$, (C) $y=2x/(2+x)$, and (D) $y=x(1+x/6)/(1+2x/3)$ (the best fit) with $y=\ln(1+x)$.

The CCM was also applied to results of determination of salicylic acid (SA) according to HPLC-MS/MS method; the quantitation is based here on comparing areas of peaks (y) obtained from mass chromatograms at different concentrations (x, mg/L) of SA, see Eq. (1). The relationships $y=y1(x; n, m)$ (Eq. (1)) were modeled here at $(n, m)=(2, 2)$, $(2, 1)$, $(1, 1)$ and $(2, 0)$, in a logarithmic scale.

Except fitting the curves obtained according to SAM and CCM, a new, integral criterion of a degree of nonlinearity of the curves fitted according to nonlinear models is suggested. For this purpose, the curves are transformed (converted) into a normalized system of variables, and put within a square with sides equal to unity. Generally, the normalization is involved here with a uniform, integral criterion of nonlinearity of curves obtained with use of different methods of analysis, within different ranges of concentrations for standard solutions, and made under different physicochemical conditions, pre-assumed in the analyses. The uniformity of normalization for CCM and SAM results from the fact that a_0, distinguishing the formulas (1) and (2), is not involved in the relations applied in the system of normalized coordinates (u, v).

All calculations made within this work were performed according to the least squares method (LSM), realized with use of Excel spreadsheet.

2. Modified standard addition method

It is assumed that N measuring flasks (V_f mL) are used. Equal volumes V_0 mL of a sample tested with unknown concentration x_0 [mg/L] of an analyte X and different volumes V_j mL ($j=1,\ldots, N$) of stock solution of X (x_S mg/L) were added into jth flask and filled up to the mark with water. Concentration of X in the jth flask is as follows:

$$x_j=\frac{x_0V_0+x_SV_j}{V_f} \tag{4}$$

Applying Eq. (4) to

$$y=y_1(x;2,2)=\frac{a_1x+a_2x^2}{1+a_3x+a_4x^2} \tag{5}$$

we get the regression equation

$$y_j=d_0+d_1V_j+d_2V_j^2+d_{11}V_jy_j+d_{21}V_j^2y_j+\varepsilon_j \tag{6}$$

where:

$$d_0=(b_1+b_2x_0V_0)x_0V_0/z;\ \ d_1=(b_1+2b_2x_0V_0)x_S/z;\ \ d_2=b_2x_S^2/z; \tag{7}$$

$$d_{11}=-(b_3+2b_4x_0V_0)x_S/z;\ \ d_{21}=-b_4x_S^2/z \tag{7a}$$

and $z=1+b_3x_0V_0+b_4x_0^2V_0^2$; $b_1=a_1/V_f$, $b_2=a_2/V_f^2$, $b_3=a_3/V_f$, $b_4=a_4/V_f^2$. Further transformations of (7) give

$$x_0=\frac{d_1x_S}{2d_2V_0}\left(1-\left(1-\frac{4d_0d_2}{d_1^2}\right)^{0.5}\right) \tag{8}$$

where d_0, d_1 and d_2 are calculated according to LSM applied to Eq. (6). Formula (8) is valid also for the functions: $y=y_1(x;\,2,1)$ and $y=y_1(x;\,2,0)$, and the function $y=y_1(x;\,2,m)$, in general, see Eq. (2) .

3. Rational functions and normalization principle

Let us refer first to the rational function

$$y=y_0(x;2,2)=\frac{a_0+a_1x+a_2x^2}{1+a_3x+a_4x^2} \tag{9}$$

applied for CCM and considered as A-model. Simplified forms of (9) are called as: B-model ($a_4=0$), C-model ($a_4=a_2=0$), and D-model ($a_4=a_3=0$); for the D-model we get the parabolic function

$$y=a_0+a_1x+a_2x^2 \tag{10}$$

Let us take the set of experimental data $\{(x_j,\,y_j)|\ j=1,\ldots,N\}$, where $x_1<x_2<\cdots<x_N$. Denoting $\Delta x=x_N-x_1$ and $\Delta y=y_N-y_1$, for a monotonic function ($y_j<y_{j+1}$ at $j=1,\ldots,N-1$), we introduce the variables u and v through the relations as follows:

$$x=x_1+u\Delta x \text{ and } y=y_1+v\Delta y \tag{11}$$

Applying them to the A-model, we get the relation

$$v=v(u)=\frac{\alpha u+\beta u^2}{1+\gamma u+\eta u^2} \tag{12}$$

where

$$\alpha=\frac{(a_1+2a_2x_1-a_3y_1-2a_4x_1y_1)}{1+a_3x_1+a_4x_1^2}\frac{\Delta x}{\Delta y} \tag{13}$$

$$\beta=\frac{a_2-a_4y_1}{1+a_3x_1+a_4x_1^2}\frac{(\Delta x)^2}{\Delta y} \tag{14}$$

$$\gamma=\frac{a_3+2a_4x_1}{1+a_3x_1+a_4x_1^2}\Delta x \tag{15}$$

$$\eta=\frac{a_4}{1+a_3x_1+a_4x_1^2}(\Delta x)^2 \tag{16}$$

Note that $v(0)=0$. At $(u,\,v)=(1,\,1)$, we have the relation

$$\alpha+\beta=1+\gamma+\eta,\ \text{ i.e. } \eta=\alpha+\beta-\gamma-1 \tag{17}$$

The parameters: a_0, …, a_4 in (13)–(16) are obtained according to LSM applied to the regression equation

$$y_j=a_0+a_1x_j+a_2x_j^2-a_3x_jy_j-a_4x_j^2y_j+\varepsilon_j \tag{18}$$

derived from Eq. (9). Note that the formulas (13)–(16) do not involve a_0; it is the basis for introducing a common criterion of nonlinearity for CCM and SAM. Moreover, the value $s=\Delta y/\Delta x$, inherent in α and β (Eqs. (13, 14)), is the mean slope of the curve expressed by Eq. (9), within the $<x_1,\,x_N>$ interval. For other models we have: (B) $\eta=0$, (C) $\eta=\beta=0$, and (D) $\eta=\gamma=0$. In these cases, Eq. (12) simplifies into the relations:

$$\text{(B)}\quad v=\frac{\alpha u+\beta u^2}{1+\gamma u}\quad(\text{where } \gamma=\alpha+\beta-1) \tag{19}$$

$$\text{(C)}\quad v=\frac{\alpha u}{1+\gamma u}\quad(\text{where } \gamma=\alpha-1) \tag{20}$$

$$\text{(D)}\quad v=\alpha u+\beta u^2\quad(\text{where } \beta=1-\alpha) \tag{21}$$

On the basis of formula (12), related to model A, or its simpler forms (19)–(21), related to models B, C and D, any set of experimental points: $\{(x_j,\,y_j)\,|j=1,\ldots,N\}$ in CCM can be presented within the frames of coordinates $(u,\,v)$, where $u\in<0,\,1>$ and $v\in<0,\,1>$, see Fig. 2. In all instances, the curve $v=v(u)$ links the points (0, 0) and (1, 1) on the $(u,\,v)$ plane. A reference is the linear

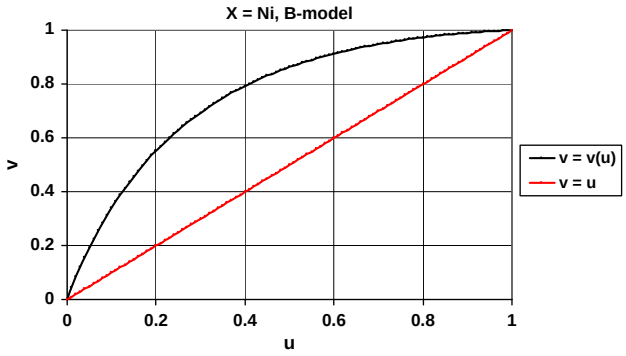

Fig. 2. The integral criterion of nonlinearity exemplified by CCM, applied for Ni measured according to FAAS, with use of B-model (see below); $\Omega_B=0.2598$ (Eq. (31)).

function $y=a_0+a_1x$ ($a_2=a_3=a_4=0$ in Eq. (9)), where we get the straight line

$$v=u \tag{22}$$

connecting the points (0, 0) and (1, 1) on the $(u,\,v)$ plane.

In order to use the formula $v=v(u)$, applicable for calculations made according to tables with elementary integrals, one can apply some transformations of Eqs. (12), (19), (20). Namely, we have for the A-model

$$v=\frac{\alpha u+\beta u^2}{1+\gamma u+\eta u^2}=\frac{\beta}{\eta}+\frac{\beta}{2\eta}\left(\frac{\alpha}{\beta}-\frac{\gamma}{\eta}\right)\frac{d}{du}\ln\left(u^2+\frac{\gamma}{\eta}u+\frac{1}{\eta}\right)-\frac{\beta}{\eta^2}\left(\frac{\gamma}{2}\left(\frac{\alpha}{\beta}-\frac{\gamma}{\eta}\right)+1\right)\frac{1}{u^2+(\gamma/\eta)u+(1/\eta)} \tag{23}$$

B-model

$$v=\frac{\alpha u+\beta u^2}{1+\gamma u}=\frac{\beta}{\gamma}u+\frac{\alpha\gamma-\beta}{\gamma^2}-\frac{\alpha\gamma-\beta}{\gamma^3}\frac{d}{du}\ln\left(u+\frac{1}{\gamma}\right) \tag{24}$$

and C-model

$$v=\frac{\alpha u}{1+\gamma u}=\frac{\alpha}{\gamma}-\frac{\alpha}{\gamma^2}\frac{d}{du}\ln\left(u+\frac{1}{\gamma}\right) \tag{25}$$

Eq. (21), referred to D-model, needs none preparatory transformation.

4. The integral criterion of nonlinearity

The area between the lines: $v=v(u)$ and $v=u$ (Eq. (22)), plotted in the normalized coordinates $(u,\,v)$, is the measure of nonlinearity of any monotonic relationship obtained on the basis of experimental points $\{(x_j,\,y_j)\,|j=1,\ldots,N\}$, compared with Fig. 1. This area is expressed as

$$\Omega=\int_0^1|v-u|du=\begin{cases}\int_0^1 v du-\frac{1}{2} & for\ v\geq u\\ \frac{1}{2}-\int_0^1 v du & for\ v\leq u\end{cases} \tag{26}$$

For the case exemplified by Fig. 1, we have $v\geq u$ within $u\in<0,\,1>$. From tables of elementary integrals [43] we have

$$\int\frac{1}{a\xi^2+b\xi+c}d\xi=\Psi(\Delta)=\begin{cases}\frac{2}{\sqrt{-\Delta}}\cdot\tan^{-1}\left(\frac{2\xi+b}{\sqrt{-\Delta}}\right) & for\ \Delta<0\\ \frac{-2}{2a\xi+b} & for\ \Delta=0\\ \frac{1}{\sqrt{\Delta}}\ln\left|\frac{2a\xi+b-\sqrt{\Delta}}{2a\xi+b+\sqrt{\Delta}}\right| & for\ \Delta>0\end{cases} \tag{27}$$

with $\Delta=b^2-4ac$. Setting $a=1$, $b=\gamma/\eta$, $c=1/\eta$ and $\xi=u$ in (27), we get

$$\Psi(\Delta)=\int_0^1\frac{1}{u^2+(\gamma/\eta)u+(1/\eta)}du$$

$$= \frac{1}{\sqrt{\Delta}} \ln \left| \frac{2\eta+\gamma-\eta\sqrt{\Delta}}{2\eta+\gamma+\eta\sqrt{\Delta}} \frac{\gamma+\eta\sqrt{\Delta}}{\gamma-\eta\sqrt{\Delta}} \right| \text{ for } \Delta > 0 \quad (28)$$

where (see Eqs. (15) and (16))

$$\Delta = \left(\frac{\gamma}{\eta}\right)^2 - \frac{4}{\eta} = \frac{a_3{}^2 - 4a_4}{(a_4 \Delta x)^2} \quad (29)$$

Then we get

$$\Omega_A = \frac{\beta}{\eta} - \frac{1}{2} + \frac{\beta}{2\eta}\left(\frac{\alpha}{\beta} - \frac{\gamma}{\eta}\right)(\ln|\alpha+\beta|) - \frac{\beta}{\eta^2}\left(\frac{\gamma}{2}\left(\frac{\alpha}{\beta} - \frac{\gamma}{\eta}\right) + 1\right)\Psi(\Delta), \text{ where } \eta = \alpha+\beta-\gamma-1 \quad (30)$$

For $\Delta > 0$, i.e. at $a_3^2 > 4a_4$ (Eq. (29)), $\Psi(\Delta)$ is expressed by Eq. (28). Similarly, from (21), (22), (24)–(26), we have (see Fig. 2)

$$\Omega_B = \frac{1-\alpha}{2\gamma} + \frac{(\alpha-1)(\alpha+\beta)}{\gamma^2}\left(1 - \frac{1}{\gamma}\ln|\alpha+\beta|\right), \text{ where } \gamma = \alpha+\beta-1 \quad (31)$$

$$\Omega_C = \frac{\alpha}{\alpha-1} - \frac{1}{2} - \frac{\alpha}{(\alpha-1)^2}\ln|\alpha| \quad (32)$$

$$\Omega_D = \frac{\alpha-1}{6} \quad (33)$$

respectively, see Eq. (21).

5. Experimental part

5.1. Apparatus and reagents

The experiments involved with potassium determination were made on an AAnalyst 200 Flame Atomic Spectrometer (PerkinElmer); this spectrometer can work according to absorption or emission mode, in air-acetylene flame. The absorption mode was applied for Ni and CCM (at 232.0 nm), whereas the emission mode was applied for K and SAM (at 766.49 nm). Multielement Cu-Fe-Ni Lumina ®Hollow Cathode Lamp (PerkinElmer) operating at 30 mA was used.

Analyses of samples with salicylic acid (SA) were made according to HPLC-MS/MS and CCM method [44]. To obtain the calibration curve for SA, full procedure designed for analyses of such samples has been applied [45]. The chromatographic analyses were made with use of an Agilent 1200 Series HPLC System (Agilent, USA) consisting on a vacuum degasser, a binary pump, an autosampler and a thermostated column compartment. Separation of SA was achieved using a Zorbax Eclipse XDB–C18 Rapid Resolution HT (4.6 × 50 mm^2 i.d.; 1.8 μm) analytical column (Agilent, USA). Elution was carried out with acetonitrile (containing formic acid 0.1%, v/v), as solvent A and aqueous 15 mmol/L ammonium formate solution (containing formic acid 0.1%, v/v) as solvent B, at a flow rate of 0.6 mL/min, with the column thermostated at 25 °C. The gradient elution program used was: 0–7 min

Table 1
Collected points in normal and logarithmic scale for experimental (exp) and calculated (calc) results obtained from the models: A, B, C and D; x – concentrations [mg/L] of SA in working solutions; y – areas of peaks registered in MS method, expressed in arbitrary units.

x	y(exp)	y(calc)				logy(exp)	logy(calc)			
		A-model	B-model	C-model	D-model		A-model	B-model	C-model	D-model
0.10	3148	3525	3339	4747	5139	3.4980	3.5472	3.5236	3.6764	3.7109
0.12	4066	4140	3983	5277	5610	3.6092	3.6171	3.6002	3.7224	3.7489
0.15	4915	5057	4940	6069	6314	3.6915	3.7039	3.6938	3.7831	3.8003
0.17	5659	5664	5572	6594	6783	3.7528	3.7532	3.7460	3.8192	3.8314
0.20	6537	6568	6512	7379	7485	3.8154	3.8174	3.8137	3.8680	3.8742
0.30	9009	9524	9569	9966	9812	3.9547	3.9788	3.9809	3.9985	3.9917
0.50	14878	15193	15369	15008	14407	4.1725	4.1817	4.1866	4.1763	4.1586
0.60	18256	17913	18125	17465	16676	4.2614	4.2532	4.2583	4.2422	4.2221
0.70	21316	20561	20793	19881	18926	4.3287	4.3130	4.3179	4.2984	4.2770
0.90	26156	25654	25888	24595	23367	4.4176	4.4091	4.4131	4.3908	4.3686
1.00	28516	28104	28325	26894	25558	4.4551	4.4488	4.4522	4.4297	4.4075
1.50	39218	39497	39560	37852	36226	4.5935	4.5966	4.5973	4.5781	4.5590
2.00	50393	49659	49508	47984	46412	4.7024	4.6960	4.6947	4.6811	4.6666
3.00	65695	67128	66652	66123	65334	4.8175	4.8269	4.8238	4.8204	4.8151
5.00	94866	94520	94231	95719	97385	4.9771	4.9755	4.9742	4.9810	4.9885
7.00	116580	116430	116945	118842	121712	5.0666	5.0661	5.0680	5.0750	5.0853
10.0	146536	146611	146468	145381	143719	5.1659	5.1662	5.1657	5.1625	5.1575

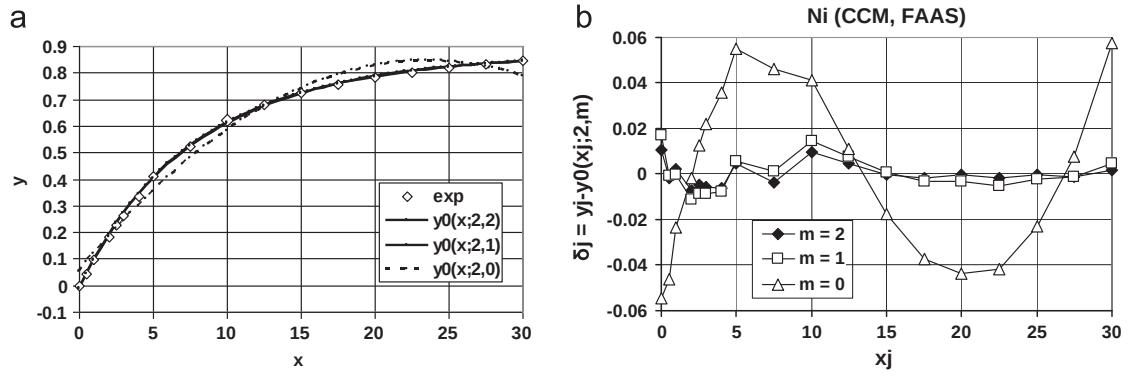

Fig. 3. Plots for Ni measured according to FAAS method: (3a) experimental points (x_j, y_j) approximated by the functions $y = y_0(x;2,m)$, $m = 0,1,2$; x – concentrations [mg/L] of Ni, $y = A$ – absorbance; (3b) the degrees of fit $\delta_j = y_j - y_j(x_j;2,m)$ of the functions at different $x = x_j$.

linear gradient, from 10% to 35% of solvent A. Mass spectrometry analyses were performed on a 6410 Triple Quadrupole (QqQ) mass spectrometer (MS) equipped with an electrospray ionization source (ESI) (Agilent, USA). Ionization of analytes was carried out using the following settings: capillary voltage: −3 kV, drying-gas flow rate: 9 L/min, drying-gas temperature 350 °C, and nebulizer pressure 40 psi. Negative ionization mode was monitored. Ions were analyzed in multiple reaction monitoring (MRM) mode. Two MRM transitions were established for SA, according to the decision [46] concerning the performance of analytical methods and interpretation of results.

All reagents were of analytical purity grade. Methanol (99.9%) or ultrapure water was used for preparation of all (stock and working) solutions.

5.2. Working solutions

5.2.1. $Ni(NO_3)_2$ solution

Nickel(II) nitrate hexahydrate for analysis (99,999%, Sigma-Aldrich) [47] was used to prepare 1.000 g/L of Ni standard solution by weighting 49,548 g of salt to prepare 1 L of solution in a volumetric flask. A working standard solution containing 125 mg/L of Ni was prepared from this standard solution. The adequate volume of working standard solution was added to 25 mL volumetric flasks to obtain the calibration standards. Measurements for each calibration solution were repeated thrice, and the absorbance at a given point was the mean value. All dilutions were made with ultrapure water.

5.2.2. KCl solution

A weighed portion 3.8326 g of KCl (99.5%, Merck) was used for preparation of 1 L of 2.000 g/L K standard solution; $3.8326 \times 39.09/74.54 \times 100/99.5 = 2.000$. A stock solution ($x_S = 100$ mg/L K) was prepared by dilution of this solution. A portion $V_W = 5$ mL of white wine (x_W mg/L K) was diluted to $V_W^* = 100$ mL and $V_0 = 1$ mL of the resulting solution (x_0 mg/L) was added into jth, $V_f = 25$ mL flask, containing V_j mL of working standard solution to obtain the spike concentrations; $x_W = 100/5x_0 = 20x_0$.

5.2.3. Salicylic acid solution

Stock solution of 10 mg/L of salicylic acid (SA) was prepared by dissolution of the preparation (> 99%, from Sigma-Aldrich (Steinheim, Germany)) in methanol (> 99.9%, from Romil (Barcelona, Spain)) and stored at 4 °C. All working solutions (see Table 1) were prepared in 1 mL flasks by dilution of portions (± 0.001 mL) of the solution to the mark with methanol. This way, the concentration range 0.10–10.0 [mg/L] of SA in working solutions taken for preparation of calibration curve was covered.

6. Results and discussion

6.1. CCM for Ni

The CCM procedure, realized with use of Eq. (1), was applied first for results for absorbance ($y = A$) measured for Ni solutions according to the FAAS method (Fig. 3a). The fit of the curves $A = A_0(x;\ 2,m)$ (Eq. (2)) for $n = 2$ and $m = 2,1,0$ is presented in Fig. 3b; the best fit occurs for $A = A_0(x;\ 2,2)$, and the worst for $A = A_0(x;\ 2,0)$. The exemplary plot, related to normalization made according to B-model ($m = 1$, Eq. (24)), is presented in Fig. 2; the value $\Omega_B = 0.2598$, calculated from Eq. (31), is the numerical value of nonlinearity related to this model.

As is apparent from Fig. 3a, black line related to $m = 2$ and $m = 1$ practically overlap. This means that the B-model is perfectly adequate. This also means that the use of models with higher m-values is quite useless, in this respect.

Curve $v = v(u)$ shows a significant degree of non-linearity expressed in Fig. 2 by the value $\Omega_B = 25.98\%$. This in turn causes the model $y = y_0(x;\ 2,0)$ inadequate, in a high degree. Moreover, a suitable curve passes through a maximum, which does not result from the arrangement of experimental points and assumption ($y_{j+1} > y_j$ or $y_{j+1} < y_j$ at $x_j + 1 > x_j$ put for $j = 1,\ldots,N-1$). Non-monotonic course of the curve $y = y_0(x,\ 2.0)$ (Fig. 3a) causes a non-monotonic course of the related curve $v = v(u)$, in Fig. 4.

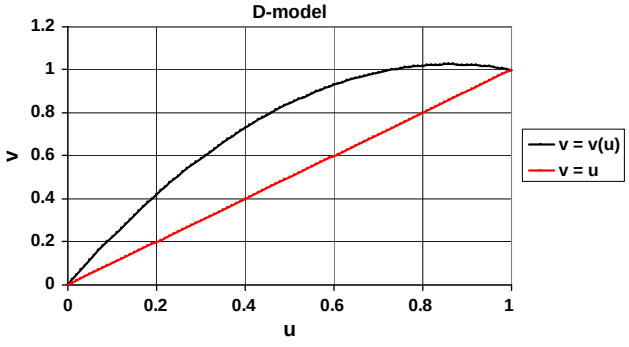

Fig. 4. Plot of $v = v(u)$ obtained from experimental data in Fig. 3; calculated $\Omega_D = 0.2293$.

6.2. SAM for K

The SAM procedure, realized with use of Eq. (2), in context with the algorithms presented above (Eq. (8)), was applied for results (Fig. 5) obtained for K measured according to FAES method. The solutions from the flasks were aspirated into the nebulizer of the

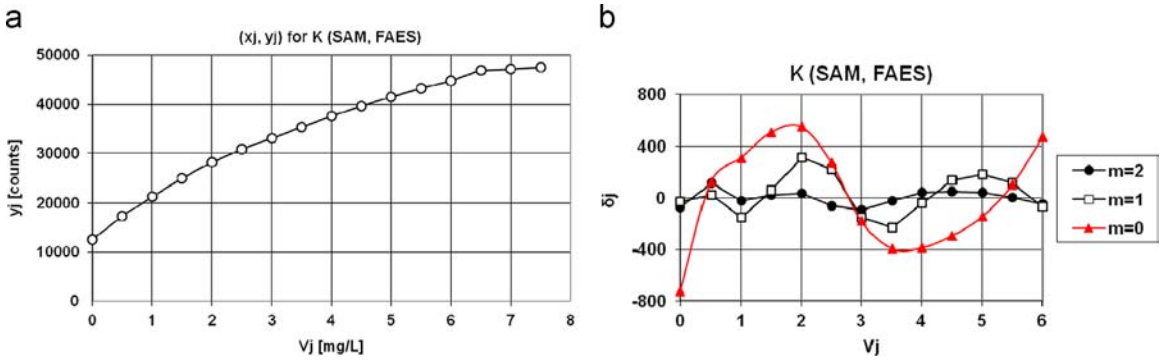

Fig. 5. The experimental points (a), and (b) the relation between $\delta_j = y_j - y_1(V_j;\ 2,\ m)$ vs. V for $y = $EI (emission intensity), at different m-values in the model given by Eq. (2) at $n = 2$ for potassium determined according to FAES method.

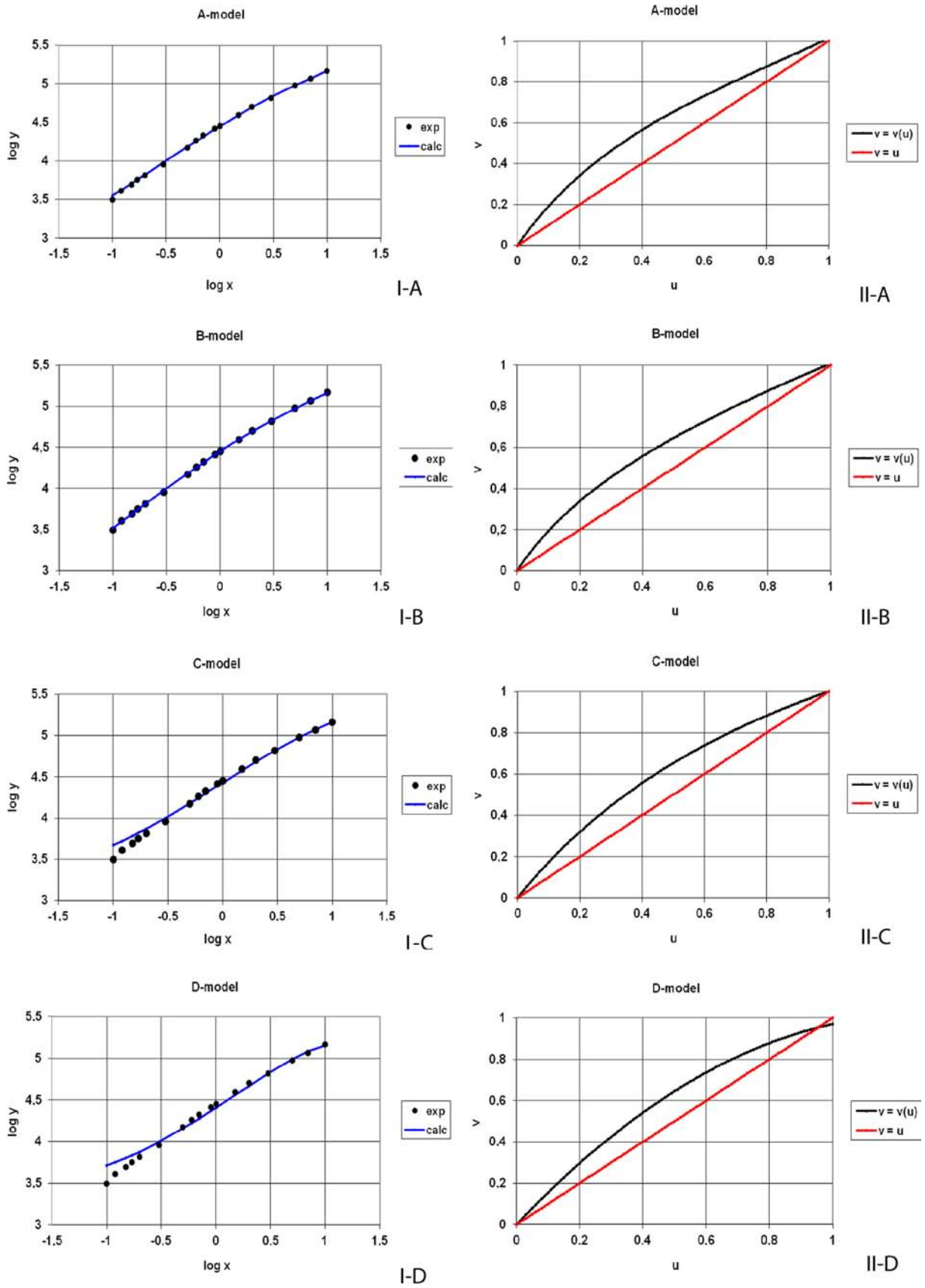

Fig. 6. I-A, I-B, I-C, I-D – experimental points $\{(\log x_j, \log y_j) | j=1,\ldots, N\}$ and curves plotted according to models A, B, C, D and II-A, II-B, II-C, II-D – plots of areas Ω_A, Ω_B, Ω_C and Ω_D between the curves $v=v(u)$ plotted according to models A, B, C and D and the line $v=u$ in the normalized system of coordinates (u, v).

spectrometer and emission intensity (EI) was measured. Signals from solutions with 26–30 mg/L K were omitted, because a warning of the instrument concerning to the saturation of the detector, i.e. the points $V \leq 6$ in Fig. 5a were involved in calculations. In the context of the degree of fit of the curves to experimental points within the V-range in Fig. 5b one can assume that the curve for $m=2$ refers to the most adequate model applicable for calculation of x_0 value. The x_0 values are there as follows: 10,782 for $m=29{,}802$ for $m=1$, and 14,903 for $m=0$. The belief that $x_0 \approx 108$ stems also from inferences arising from the course of the curves in Fig. 1, and from the literature data [30].

6.3. CCM for salicylic acid

Salicylic acid (SA), as the main metabolite of aspirin (acetylsalicylic acid), is one of contaminants in surface waters. Analysis of SA samples according to HPLC-MS/MS was made as presented above. SA is readily ionized under soft ESI conditions to yield the deprotonated $[M–H]^-$ ion at m/z 137.1 Da, in the negative mode. Upon collision-induced dissociation (CID), a major product ion at m/z 93.1 Da is observed that corresponds to the loss of CO_2: $C_6H_5(OH)COO^- = C_6H_5OH^{\cdot} + CO_2$. This transition of 137.1 Da (precursor ion) to 93.1 Da (the fragmentation ion, with the highest response) is commonly selected for quantification purposes of SA based on (HPLC-MS/MS) tandem mass spectrometry (QqQ-MS). Conditions of the analysis: fragmenter 80 V, and collision energy 15 eV.

The results of measurements, presented in Table 1, with integrated areas (y_j) of the related peaks obtained from a series of $N=17$ working SA solutions, with concentrations x_j covering the range 0.1–10 mg/L SA, are presented in the first (I) column of Fig. 6 in logarithmic scale, $\{(\log x_j, \log y_j) | j=1,\ldots, N\}$, together with the approximating lines, referred to models A, B, C and D. It is stated that the curves related to models A and B fit the experimental points quite satisfactorily; only at lowest SA concentrations, the approximation is not so good. The sum of squares $SS = \sum_{j=1}^{17} (\log y_j(\exp) - (\log y_j(calc))^2$ is equal to: 0.0039 for A, 0.0019 for B, 0.0656 for C and 0.0998 for D, i.e. the approximations of the models C and D are much worse. This demonstrates the usefulness of the models A and B. Application of rational functions $y=y(x; n, m)$ with higher n and m values is not suggested.

The curves $y=y(x; n, m)$ approximating the experimental points $\{(x_j, y_j) \mid j=1,\ldots, N\}$ appear clearly non-linear course, expressed by the values: $\Omega_A=0.1086$, $\Omega_B=0.1056$, $\Omega_C=0.1041$, $\Omega_D=0.1016$ obtained from the models A, B, C and D, respectively (Eqs. (30)–(33)). The related graphs are shown in the second (II) column in Fig. 6. Similarity in Ω-values, within ca. 10%, means that the mismatch between the experimental points and respective approximating function visible in the column I does not translate into a significant effect on the Ω-value that expresses the respective area in the column II. This is due to the fact that this mismatch has essentially a place for low x-values, where the appropriate signal y is relatively small.

7. Final comments

In this paper, the new formulation based on application of the rational functions $y=y(x; n,m)$ of the Padé type (Padé appoximants, Eqs. (1, 2)) is presented in context with calibration curve (CCM) and standard addition (SAM) methods. It was found that the Padé approximants are far more applicable than polynomial functions when applied for modeling purposes. A uniform criterion of nonlinearity of the functions obtained in CCM and SAM is also presented. This criterion is based on the calculation of area Ω between the lines $v=v(u)$ and $v=u$ within the unit plane of normalized variables (u, v). The usefulness of this approach was tested on three different methods of spectrometric analyses.

Calibration curves in the system considered are characterized by a high degree of non-linearity. The numerical value of the area Ω does not depend significantly on the misfit of calibration curve at lower concentrations. This normalization provides a uniform, integral criterion of nonlinearity of curves obtained with use of different methods of analysis, within different ranges of concentrations assumed for standard solutions, and made under different physicochemical conditions pre-assumed in the analysis. It appears to be far more general and more robust than the approaches to nonlinearity criteria suggested elsewhere [48] (see also references cited therein).

References

[1] H. Padé, J. Math. Pures Appl 10 (1894) 291–329.
[2] C. Brezinski, Appl. Numer. Math. 20 (1996) 299–318.
[3] W.H. Press, S.A. Teukolsky, W.T. Vetterling, B.P. Flannery, Numerical Recipes: The Art of Scientific Computing, Cambridge University Press, Cambridge (2007) 2007124–127.
[4] R.F. Heiser, W.R. Parrish, Ind. Eng. Chem. Res. 28 (1989) 484–489.
[5] E. Hernández-Pacheco, M.D. Mann, J. Power Sources 128 (2004) 25–33.
[6] J. Bartkovjak, M. Karovičová, Meas. Sci. Rev. 1 (2001) 63–65.
[7] T. Michałowski, Chem. Anal. 26 (1981) 799–813.
[8] T. Michałowski, M. Toporek, M. Rymanowski, Talanta 65 (2005) 1241–1253.
[9] T. Michałowski, A. Baterowicz, A. Madej, J. Kochana, Anal. Chim. Acta 442 (2001) 287–293.
[10] T. Michałowski, K. Kupiec, M. Rymanowski, Anal. Chim. Acta 606 (2008) 172–183.
[11] M. Ponikvar, T. Michałowski, K. Kupiec, S. Wybraniec, M. Rymanowski, Anal. Chim. Acta 628 (2008) 181–189.
[12] T. Michałowski, B. Pilarski, M. Ponikvar-Svet, A.G. Asuero, A. Kukwa, J. Młodzianowski, Talanta 83 (2011) 1530–1537.
[13] T. Michałowski, A. Rokosz, A. Tomsia, Analyst 112 (1987) 1739–1741.
[14] T. Michałowski, Analyst 113 (1988) 833–935.
[15] T. Michałowski, A. Rokosz, E. Negrusz-Szczęsna, Analyst 113 (1988) 969–972.
[16] T. Michałowski, A. Rokosz, P. Kościelniak, J.M. Łagan, J. Mrozek, Analyst 114 (1989) 1689–1692.
[17] T. Michałowski, Talanta 39 (1992) 1127–1137.
[18] T. Michałowski, E. Gibas, Talanta 41 (1994) 1311–1317.
[19] T. Michałowski, A. Rokosz, M. Zachara, Chem. Anal. (Warsaw) 39 (1994) 217–222.
[20] A.G. Asuero, T. Michałowski, Crit. Rev. Anal. Chem. 41 (2011) 151–187.
[21] T. Michałowski, A.G. Asuero, Crit. Rev. Anal. Chem. 42 (2012) 220–244.
[22] N. Damil, M. Potier-Ferry, A. Najah, R. Chari, H. Lahmam, Commun. Numer. Meth. Eng. 15 (1999) 701–708.
[23] T. Michałowski, in: T. Michałowski (Ed.), Applications of MATLAB in Science and Engineering, InTech – Open Access Publisher in the fields of Science, Technology and Medicine, Rijeka, Croatia, 2011, pp. 1–34 ⟨http://www.intechopen.com/books/show/title/applications-of-matlab-in-science-and-engineering⟩ (Chapter 1).
[24] F.S. Acton, Numerical Methods That Work, Harper & Row, New York, 1970.
[25] B. Pilarski, A. Dobkowska, H. Foks, T. Michałowski, Talanta 80 (2010) 1073–1080.
[26] V.-M. Taavitsainen, A. Lehtovaara, M. Lähteenmäki, J. Chemom. 24 (2010) 505–513.
[27] P. Ingelstrom, L. Lindholm, T. Rylander, Int. J. Numer. Model 16 (2003) 287–298.
[28] S. Dhatt, K.J. Bhattacharyya, J. Math. Chem. 51 (2013) 1467–1477.
[29] V-M. Taavitsainen, Chemom. Intell. Lab. Syst. 120 (2013) 136–141.
[30] W.B. Barnett, Spectrochim. Acta 39B (1984) 829–836.
[31] T. Kakiuchi, H. Usui, D. Hobara, M. Yamamoto, Langmuir 18 (2002) 5231–5238.
[32] D.I. Mendoza-Castillo, A. Bonilla-Petriciolet, J. Jáuregui-Rincon, Afinidad LXVII 547 (2010) 203–211.
[33] A.I. Oleinicke, D. Battistel, S. Daniele, I. Svir, C. Amatore, Anal. Chem. 83 (2011) 4887–4893.
[34] L. Rajendran, Electrochim. Acta 51 (2006) 5407–5411.
[35] J-P. Diard, B. le Gunet, C. Montella, J. Electroanal. Chem. 584 (2005) 182–191.
[36] K. Gorazda, A.M. Michałowska-Kaczmarczyk, A.G. Asuero, T. Michałowski, Talanta 116 (2013) 927–930.
[37] T. Michałowski, B. Pilarski, A.M. Michałowska-Kaczmarczyk, A. Kukwa, Talanta 124 (2014) 36–42.
[38] P. Kościelniak, Chemom. Intell. Lab. Syst. 47 (1999) 275–287.
[39] Analytical Methods for Atomic Absorption Spectroscopy, The Perkin-Elmer Corporation, 1996.
[40] OIV Compendium of International Methods of Wine and Must Analysis, Potassium, Method OIV-MA-AS322-02B: R 2009, International Organization of Vine and Wine, Edition 2012, Volume 2, Paris, 2014.
[41] G. Grindlay, J. Mora, L. Gras, M.T.C. de Loos-Vollebregt, Anal. Chim. Acta 691 (2011) 18–32.

[42] M. Aceto, O. Abollino, M.C. Bruzzoniti, E. Mentasti, C. Sarzanini, M. Malandrino, Food Addit. Contam. 19 (2002) 126–133.
[43] I.N. Bronštejn, K.A. Semendjajev, A Guide-Book to Mathematics for Technologists and Engineers, Pergamon, Oxford, 1964.
[44] B. Kasprzyk-Hordern, R.M. Dinsdale, A.J. Guwy, Anal. Bioanal. Chem. 391 (2008) 1293–1308.
[45] D. Camacho-Muñoz, J. Martin, J.L. Santos, I. Aparicio, E. Alonso, J. Sep. Sci. 32 (2009) 3064–3073.
[46] Commission Decision 2002/657/EC implementing Council Directive 96/23/EC. Official Journal of the European Union L 125, 23 May, 1996, pp. 10–32.
[47] ⟨http://www.sigmaaldrich.com/catalog/product/aldrich/203874?lang=pl&region=PL⟩, 2014.
[48] K. Emancipator, M.H. Kroll, Clin. Chem. 39 (1993) 766–772.